

Map-Based Neuron Networks

Borja Ibarz^{*}, Hongjun Cao^{†,*} and Miguel A. F. Sanjuán^{*}

^{*}*Nonlinear Dynamics and Chaos Group, Departamento de Ciencias de la Naturaleza y Física Aplicada, Universidad Rey Juan Carlos, Tulipán s/n, 28933 Móstoles, Madrid, Spain*

[†]*Department of Mathematics, School of Science, Beijing Jiaotong University, Beijing 100044, P. R. China*

Abstract.

Ever since the pioneering work of Hodgkin and Huxley, biological neuron models have consisted of ODEs representing the evolution of the transmembrane voltage and the dynamics of ionic conductances. It is only recently that maps – or difference equations – have begun to receive attention as valid conductance neuron models. They can not only be computationally advantageous substitutes of ODE models, but, since they accommodate chaotic dynamics in a natural way, they may reproduce rich collective behaviors that we explore here.

Keywords: map-based model, neuron networks, collective behavior, synchronization

PACS: 05.45.-a, 05.45.Xt, 87.18.Sn, 87.19.La, 89.75.F6

SIMPLE MAP-BASED NEURON MODELS

One of the simplest conductance-based neuron models is the leaky integrate-and-fire (LIF) model [1]. It represents the voltage v across a capacitor (the cell membrane) that passively discharges through a resistor (the ionic channels) and may be charged by external currents (either injected or generated by synaptic events). If voltage reaches a threshold v_θ , the capacitor instantaneously discharges to a reset level v_r and the neuron is said to have fired a spike. The equations that represent this model are:

$$\begin{aligned} C\dot{v}(t) &= -\frac{v(t)}{R} + I_{ext}(t) \\ v(t^+) &= v_r \quad \text{if } v(t^-) = v_\theta \text{ (spike generation).} \end{aligned} \quad (1)$$

Observe that the model sets the resting potential of the neuron at $v = 0$. Resistance R may be dependent on v , giving rise to nonlinear LIF models. For most applications we can integrate this model with the simplest Euler method using an appropriate time step¹ (less than the typical spike duration, that is, 1 ms) to obtain a discrete-time, or map-based system:

$$v(t+1) = f(v(t)) + rI \quad \text{where } f(v) = \begin{cases} (1-k)v & \text{if } v < v_\theta, \\ v_s & \text{if } v_\theta < v < v_s, \\ v_r & \text{if } v = v_s. \end{cases} \quad (2)$$

¹ Euler integration needs extremely small time steps to avoid significant errors with respect to the exact solution of a network of ODE-based LIF neurons, especially due to the round-off of the threshold crossing time [2]; but never lose sight that the ODE-based LIF model is itself a rough approximation to real neurons. Time discretization is valid as long as it is significantly finer than the highest frequency in the system.

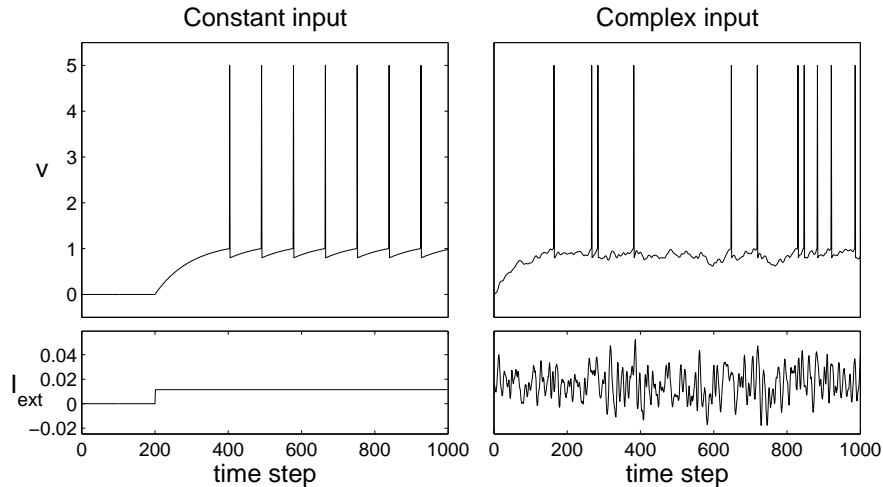


FIGURE 1. Response of a LIF neuron to a constant external current (left) and a complex external current (right). Parameters in Eqs. (2) are $k = 0.01$, $r = 1$, $v_\theta = 1$, $v_r = 0.8$ and $v_s = 5$.

Parameter correspondence is $k = \frac{\Delta t}{RC}$ and $r = \frac{\Delta t}{C}$, where Δt is the integration time step. A slight modification with respect to continuous time is that this discrete-time model explicitly represents spikes as a (high) voltage value v_s , and that the spike occupies a finite one time step interval. Observe that the mapping $f(v)$ includes both the subthreshold resistor and the spike generation; seamless incorporation of threshold and reset mechanisms is a convenient feature of map-based models.

Although simple, models of the LIF family are able to reproduce the response of complex models and even real neurons to currents injected in their soma [3]. Although the autonomous behavior of the LIF model (i.e., when I is a fixed parameter) is either a constant subthreshold voltage (quiescent or silent regime) or periodic firing (regular spiking regime), depending on whether I is low or high, its response under complex stimulation, as we can see in Fig. 1, looks rich and natural. Such stimulation can be generated by a large network of LIF neurons [4]. Thus, simple models are often an excellent choice for studying phenomena depending mostly on network effects rather than single neuron properties.

But in many instances the autonomous dynamics of the model needs to account for phenomena such as oscillations below the firing threshold, resonance or bursting. LIF neurons cannot display these properties because they are one-dimensional. A second variable can provide the necessary mechanism. The following equations describe a generic simple two-dimensional map-based model:

$$\begin{aligned} v(t+1) &= f(v(t)) + I - u(t), \\ u(t+1) &= u(t) + \mu(av(t) - bu(t) + \sigma). \end{aligned} \quad (3)$$

The voltage equation is that of a LIF model, and $f(v)$ includes thresholding to generate spikes; the parameter r of Eqs. (2) has been made 1 by appropriate scaling of I . The second variable enters the voltage dynamics simply as an additional current term (the minus sign means that positive u values have an inhibitory effect and viceversa, but

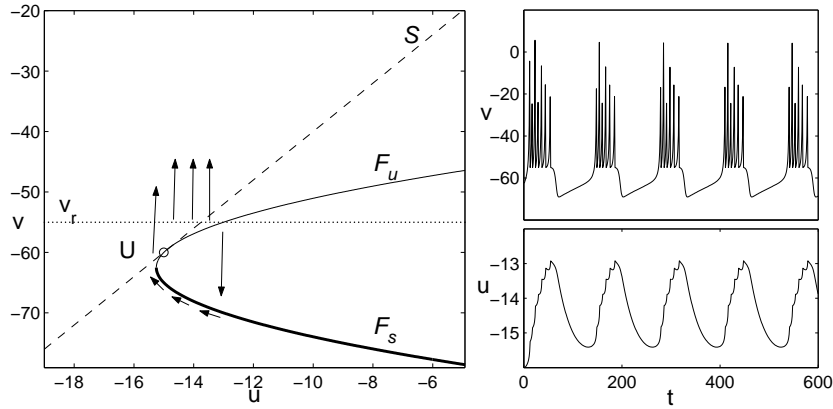


FIGURE 2. Left: nullcline diagram of the Izhikevich neuron model [8]. The slow nullcline S , and the stable and unstable branches, F_s and F_u , of the fast nullcline are represented, along with the (unstable) fixed point U . The dotted line marks the reset voltage v_r . Arrows indicate the direction of the flow. Right: time evolution of the system. Parameter values in Eqs. (3) are $\mu = 0.02$, $a = 0.25$, $b = 1$ and $I = 1$.

this is of little relevance). It represents the current due to voltage-dependent channels that evolve in the same or in a slower time scale than the voltage itself, as opposed to channels embodied in the (possibly nonlinear) resistor, which respond instantaneously to voltage changes. The time scale can be set by means of parameter μ . If it is small, u is a slow variable; this is typical of bursting models [5], which will be our main concern in this paper. In the general case, with u as fast as v , we get the so-called resonate-and-fire [6] or generalized integrate-and-fire [7] models, which exhibit interesting frequency responses.

How does a bursting model work? First observe the voltage equation in (3): when u is high, the total current term is low and the neuron is silent. When u is low, the opposite is true and the neuron is spiking. But according to the $u(t)$ equation, if $a > 0$ and σ is appropriately chosen, the low value of $v(t)$ in the quiescent state may decrease u (slowly since μ is small) until the neuron begins to fire. And, conversely, the higher average value of $v(t)$ during spiking may increase u until it draws the neuron back into silence. This alternation of spiking and silent phases is what we call bursting. The mechanism can be seen at work in Fig. 2, where the nullcline diagram and the time evolution of the well-known map-based neuron model proposed by E. M. Izhikevich [8] are depicted. See how u builds up during the spiking phase to a value where the reset voltage ($v_r = -55$ in this example) is below the unstable branch of the fast nullcline F_u ; this terminates the burst, and then u relaxes back to trigger the next one.

As with one-dimensional LIF models, $f(v)$ can be chosen in many different ways to give as many different models. Two interesting choices are shown in Fig. 3 as return maps of $v(t)$. The first one is a typical nonlinear integrate-and-fire map, and corresponds to a model proposed by N. Rulkov [9]. The two fixed points of the map, one stable and the other unstable, would appear as part of F_s and F_u in a nullcline diagram such as that of Fig. 2. Increases in the external current I or decreases in u displace this return map upwards and may eliminate the fixed points altogether, producing repetitive spiking. Observe the threshold and reset mechanism embodied in the horizontal parts of the

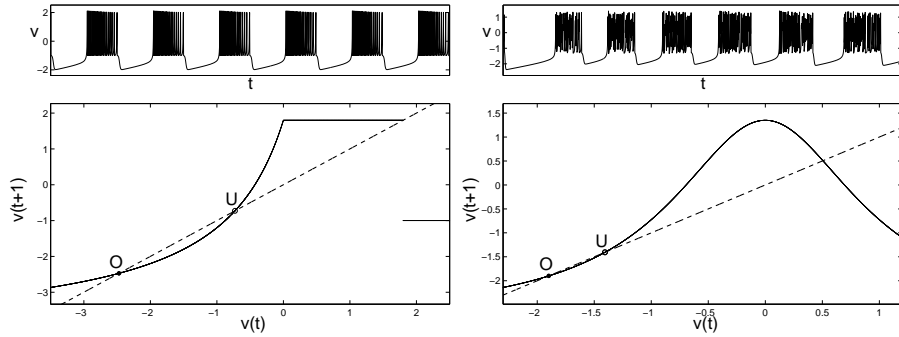


FIGURE 3. Fast variable return maps (below) and examples of bursting (top) for two different choices of $f(v)$ in Eqs. (3): left, the Rulkov map [9]; right, the chaotic Rulkov map [11]. O , stable fixed point; U , unstable fixed point. Note the irregular length of the bursts of the chaotic map.

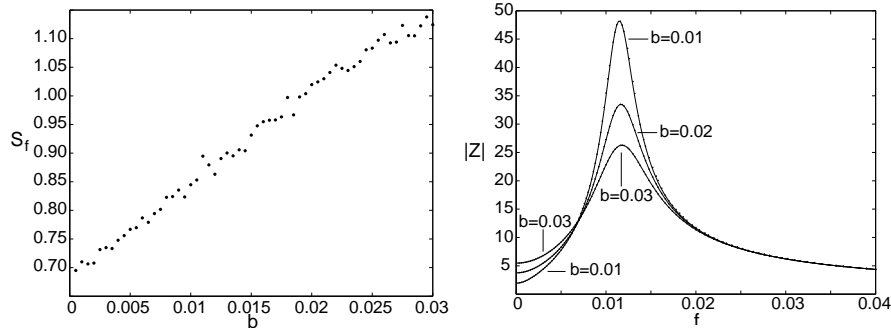


FIGURE 4. Left: sensitivity of the Izhikevich model [8] as a function of parameter b in Eqs. (3). Right: impedance curves for different values of b . For details, see [12].

return map. The second example interestingly substitutes them with a unimodal chaotic map. The reset level now varies with each spike and the result are chaotic bursts. The possibility of such simple chaotic bursting neurons is another advantage of map-based models [10, 11].

Finally we point out the relevance of parameters a and b in Eqs. (3). They determine the slope, b/a , of the slow nullcline. If $b/a = 0$, the nullcline is horizontal and u is a neutrally stable variable. The neuron is most insensitive in this state to steady changes in external current. This can be understood noting that the effect of I is to shift the fast nullcline horizontally; if the slow nullcline is horizontal, no change results in the steady state of the system. In return, the smaller the value of b/a , the sharper the frequency selectivity of the neuron. Thus a and b allow us to tune the neuron between integrator and resonator behaviors [5]. This flexibility is not available in one-dimensional models. Figure 4 shows how sensitivity grows with growing b , while resonance is enhanced for low b values [12].

FROM NEURONS TO NETWORKS

When neurons form networks, the firing activity of each of them induces currents in their postsynaptic targets. Synapses are either electrical or chemical. Electrical synapses are usually modelled by straightforward resistive coupling. Chemical synapses are instead varied and complex. In keeping with the spirit of simplification of our models, we will use instantaneous thresholded coupling of the voltage. This means that, whenever the voltage of the presynaptic neuron is above a certain threshold, it will induce in its postsynaptic targets an ohmic current. Thus we arrive at the following equations for a network of N map-based neurons with electrical and chemical connections:

$$\begin{aligned} v_n(t+1) &= f_n(v_n(t)) + I - u(t) + \sum_1^N g_{mn}^e [v_m(t) - v_n(t)] + \sum_1^N g_{mn}^c H(v_m(t) - \theta_{mn}) \\ u_n(t+1) &= u(t) + \mu_n(a_n v(t) - b_n u(t) + \sigma_n). \end{aligned} \tag{4}$$

Here $H(x)$ is the Heaviside step function and θ_{mn} is the voltage threshold for chemical synaptic interaction from neuron m to neuron n ; this threshold is usually taken just below spike initiation voltage. The coefficients g_{mn}^e and g_{mn}^c are the strengths of electrical and chemical synapses. Electrical coupling satisfies $g_{mn}^e > 0$ and $g_{mn}^e = g_{nm}^e$, and directly adds another current term to the voltage equation. Chemical coupling coefficients can be both positive (excitatory synapses) or negative (inhibitory synapses), are usually asymmetrical, and may exert their influence in any of the two equations; the choice in Eqs. (4) means that chemical synapses act on fast ion channels, but if we want to model slower synaptic dynamics we may include this term in the equation for u .

In Fig. 5 a ring of chaotic Rulkov neurons can be seen in action. Neighbors are coupled through uniform electrical synapses of strength $g^e > 0$ and inhibitory chemical synapses of strength $g^c < 0$. When a neuron begins to fire, the electrical coupling draws its silent neighbors towards higher voltages and causes them to burst. But then the inhibitory chemical coupling becomes active and hinders the neighbors' bursts. Thus the two couplings are antagonistic. Linear analysis techniques show that, in any regular network of this kind of neurons, if $g^e > |g^c|$ neurons will end up bursting synchronously [13].

If $g^e < |g^c|$, a bursting neuron prevents its neighbors from bursting, and, as depicted at the top part of Fig. 5, antiphase synchronization may appear. But, the neurons being chaotic, other configurations are possible, including propagation of waves at different speeds and directions. If electrical and chemical strengths are almost balanced, these configurations alternate unpredictably as shown in the bottom part of Fig. 5. This phenomenon is called chaotic itinerancy [14].

Obviously, the structure of the network is at least as important as the properties of individual neurons and synapses in determining the patterns of neuronal activity that will set in. The relationship between network topology and synchronization, clustering or information processing has been subject of extensive research, and all the tools that have been developed in the frame of ODE-based systems, such as mean-field theory [15], master stability functions [16] or the connection graph method [17], are available for our maps. Particular interesting situations arise in networks of mutually inhibitory bursting neurons such as those of central pattern generators [18], [19]. A simple but nontrivial example is shown in Fig. 6, where the activity in a 4×4 bidimensional lattice of inhibitory Rulkov neurons [9] is depicted for different values of inhibitory chemical

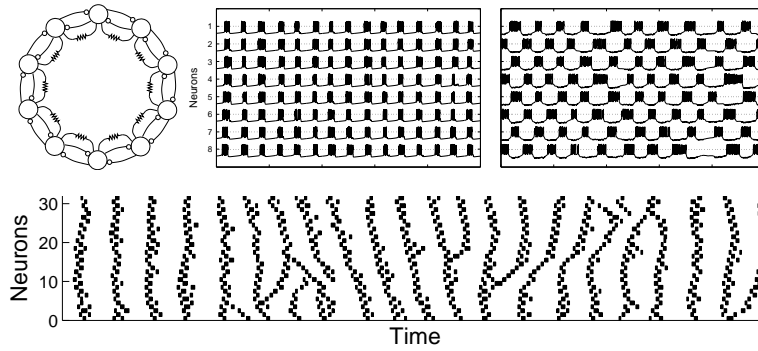


FIGURE 5. Top: a ring of chaotic Rulkov neurons [11] with electrical and inhibitory chemical coupling. The evolution of the voltage of 8 neurons is shown in the case when electrical synapses are stronger (left) or weaker (right) than chemical synapses. Note the irregular length of the bursts. Bottom: with chemical inhibition $g^c = 0.02$ and electrical coupling $g^e = 0$, a ring of 32 neurons presents rich itinerant dynamics. Parameters for Eqs. (3) are $\mu = 0.001$, $a = 1$, $b = 0$ and $I = 0$; $f(v)$ as in [11] with $\alpha = 4.3$.

coupling g^c (the coupling enters in this case the slow variable equation). Observe how the coupling strength selects the pattern of active neurons according to the symmetries of the network, and that intermediate inhibition values drive the whole system into silence. Thus neurons form dynamic patterns of activity that can be selected by synaptic parameters.

FURTHER DIRECTIONS

The map-based neurons we have presented here fall into the class of conductance-based models. They are fast simplified counterparts of the classical ODE models of the Hodgkin-Huxley type based on ionic conductances. We have seen how considering

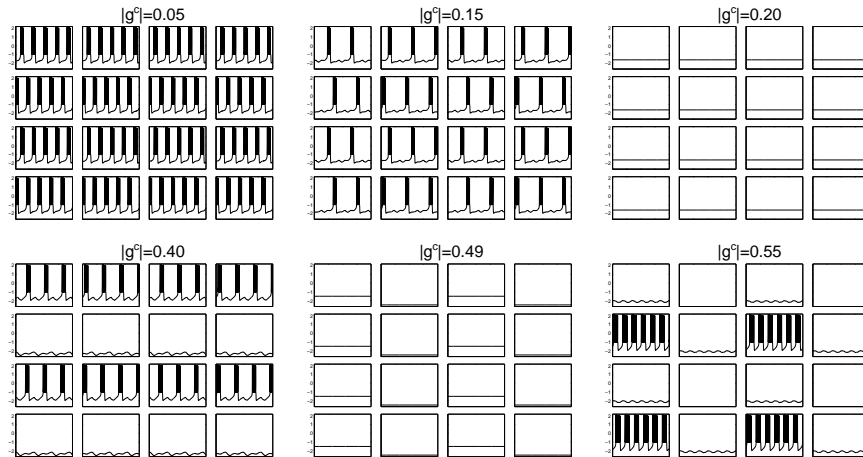


FIGURE 6. Patterns of synchronization of a homogeneous 4×4 lattice of Rulkov neurons for different values of chemical inhibitory coupling g^c

the threshold-and-reset mechanism as a discontinuous return map suggested using other maps for spike generation (see Fig. 3) and opened the door to new neuron models. We have not addressed non-conductance-based neuron models, such as the one proposed by Aihara [20], that focus on the effects of refractoriness and graded response on spike sequence generation. They are an interesting bridge between biological and formal neurons, but have never been used in modelling of biological systems. In addition, the effect of symmetry-breaking phenomenon on the generation and synchronization of bursts has been discussed in our recent work [21].

We have mentioned the computational advantage of map-based conductance neuron models only in passing. One may certainly use these models to perform large scale simulations in modest computers, gaining some edge over their slower ODE-based counterparts [22]. This has only marginal importance. Map-based models should be taken into consideration for modelling in neuroscience when they capture the features that are thought to be essential to the issue under study; if satisfactory explanations of phenomena are obtained, then they should be checked with more accurate models.

ACKNOWLEDGMENTS

This work is supported by the Spanish Ministry of Science and Technology under project number BFM2003-03081 and the Program of Mobility of Foreign Researchers by the State Secretary of Universities and Research of the Spanish Ministry of Education and Science under the project number SB2004-002 (H. Cao).

REFERENCES

1. W. Gerstner, and W. M. Kistler, *Spiking neuron models*, Cambridge University press, 1999.
2. D. Hansel, G. Mato, C. Meunier, and L. Neltner, *Neur. Comp* **10**, 467–483 (1998).
3. R. Jolivet, A. Rauch, H. R. Luscher, and W. Gerstner, *J. Comp. Neurosci*, **21**, 35–49 (2006).
4. M. V. Tsodyks, and T. Sejnowski, *Comp. in Neural Systems*, **6**, 111–124 (1994).
5. E. M. Izhikevich, *Int. J. Bifurcation Chaos Appl. Sci. Eng.*, **10**, 1171–1266 (2000).
6. E. M. Izhikevich, *Neural Networks*, **14**, 883–894 (2001).
7. M. J. E. Richardso, N. Brunel, and V. Hakim, *J. Neurophysiol.* **89**, 2538–2554 (2003).
8. E. M. Izhikevich, *IEEE Trans. Neural Networks*, **14**, 1569–1572 (2004).
9. N. F. Rulkov, *Phys. Rev. E*, **65**, 041922 (2002).
10. D. R. Chialvo, *Chaos, Solitons and Fractals*, **5**, 461–479 (1995).
11. N. F. Rulkov, *Phys. Rev. Lett*, **86**, 183–186 (2001).
12. B. Ibarz, G. Tanaka, M. A. F. Sanjuán, and K. Aihara, *Phys. Rev. E*, (submitted) (2006).
13. G. Tanaka, B. Ibarz, M. A. F. Sanjuán, and K. Aihara, *Chaos*, **16**, 013113 (2006).
14. K. Kaneko, and I. Tsuda, *Chaos*, **13**, 926–936 (2003).
15. D. J. Amit, and N. Brunel, *Cereb. Cortex*, **7**, 237–252 (1997).
16. L. M. Pecora, and T. L. Carroll, *Phys. Rev. Lett*, **80**, 2109–2112 (1998).
17. V. N. Belykh, I. V. Belykh, and M. Hasler, *Physica D*, **195**, 159–187 (2004).
18. E. Marder, and D. Bucher, *Curr. Biol*, **11**, R986–R996 (2001).
19. J. M. Casado, B. Ibarz, and M. A. F. Sanjuán, *Modern Phys. Lett. B*, **18**, 1347–1366 (2004).
20. K. Aihara, T. Takabe, and M. Toyoda, *Phys. Lett. A*, **144**, 333–340 (1990).
21. H. Cao, B. Ibarz, G. Tanaka, and M. A. F. Sanjuán, *Phys. Rev. E*, (submitted) (2006).
22. N. F. Rulkov, I. Timofeev, and M. Bazhenov, *J. Comp. Neurosci*, **17**, 203–223 (2004).